

# The nature of the intra-night optical variability in blazars

R. Bachev,<sup>1\*</sup> E. Semkov,<sup>1</sup> A. Strigachev,<sup>1</sup> Alok C. Gupta,<sup>2</sup> Haritma Gaur,<sup>2,3</sup>  
B. Mihov,<sup>1</sup> S. Boeva<sup>1</sup> and L. Slavcheva-Mihova<sup>1</sup>

<sup>1</sup>*Institute of Astronomy and National Astronomical Observatory, Bulgarian Academy of Sciences, Sofia 1784, Bulgaria*

<sup>2</sup>*Aryabhata Research Institute of Observational Sciences (ARIES), Manora Peak, Nainital – 263129, India*

<sup>3</sup>*Department of Physics, DDU Gorakhpur University, Gorakhpur – 273009, India*

Accepted 2012 May 14. Received 2012 May 11; in original form 2012 March 27

## ABSTRACT

In this paper we present the results of a short-term optical monitoring program of 13 blazars. The objects were monitored mostly in the *R* band for a total of  $\sim 160$  h between 2006 and 2011. We study the nature of the short-term variations and show that most of them could be described as slow, smooth and (almost) linear changes of up to  $\sim 0.1$  mag  $\text{h}^{-1}$ , but that many objects show no short-term variations at all. In fact, we found only a  $\sim 2$  per cent chance of observing variability of more than  $0.1$  mag  $\text{h}^{-1}$  for the sample we observed. Hints of quasi-periodic oscillations at very low-amplitude levels are also found for some objects. We briefly discuss some of the possible mechanisms for generating the intra-night variability and the quasi-periodic oscillations.

**Key words:** BL Lacertae objects: general.

## 1 INTRODUCTION

It is now widely accepted that a large variety of observational blazar phenomena, including the powerful emission, the spectral energy distribution (SED) covering practically all energy bands, the exceptional variability and the strong polarization, can be attributed to plasma processes in a relativistic jet. According to the commonly invoked scheme, a highly relativistic jet, directed at a small angle with respect to the line of sight (Urry & Padovani 1995), generates most of the observed spectrum via synchrotron and inverse Compton processes. Owing to the relativistic beaming, the emission is highly anisotropic, significantly amplified, and frequency-shifted with a typical bulk Doppler factor ( $\delta$ ) of around 10–30, as assessed by the SED modelling or variability properties (Hovatta et al. 2009; Wu et al. 2011b; Rani et al. 2011a).

As active galactic nuclei (AGN) that are not dominated by jets generally do not show huge variations, at least not on intra-night time-scales, it is almost certain that the blazar variability is associated with the processes in the relativistic jet (see Wagner & Witzel 1995 for a review). These processes could be intrinsic to the jet and related to a change of the jet power, for instance. The jet power will change as a result of the rapid evolution of the energy spectrum of the emitting relativistic particles owing either to energy loss (both synchrotron and Compton losses) or to energy gain (re-acceleration or fresh particle injection), or to both at different scales. The pro-

cesses responsible for the variations could also be related to the jet geometry; that is, to a changing jet direction (a curved or swinging jet; Gopal-Krishna & Wiita 1992) leading to a variable bulk Doppler factor of the blobs travelling along the jet. The last type of process generates observable variability even if no change of the overall jet power occurs. Finally, the variability could be caused by entirely extrinsic processes, such as microlensing (Gopal-Krishna & Subramanian 1991; Paczynski 1996) from intervening objects (e.g. stars in a foreground galaxy) along the line of sight. Thus, the emission from blobs moving relativistically down the jet might vary as a result of microlensing at a much faster rate than what is normally expected. Furthermore, the jet itself is not a stationary object: a number of phenomena, including turbulence, developing/decaying shocks, various instabilities and changing environment, could cause variability, at least on longer time-scales.

It is, therefore, not surprising that the exact cause of blazar variability is still under debate. A solution to this problem is, however, important beyond the field of astrophysics. Understanding blazar variability is one of the keys to understanding the physical processes in a relativistic jet. Because jets are natural accelerators to energies exceeding by many orders what can be achieved on Earth, blazar studies could also be of extreme importance for understanding the fundamentals of physics.

This work focuses on optical variations on the shortest time-scales (the so-called intra-night or intra-day variability). Optical studies are very important for blazars, as even though their spectrum is very broad, a key ingredient of their SED, namely the synchrotron peak, is often located close to these wavelengths.

\*E-mail: bachevr@astro.bas.bg

Although time-costly, intra-night variability studies cannot be replaced by *inter*-night (long-term) monitoring, as the short-term magnitude gradients are often much larger than night-to-night gradients (see, for instance, fig. 1 in Romero, Cellone & Combi 2000; fig. 2 in Cellone, Romero & Araudo 2007). Fortunately, most of the objects can be successfully monitored with relatively small-class (<1-m) telescopes, making it possible to organize dense, multisite monitoring of selected objects (e.g. WEBT/GASP campaigns<sup>1</sup>).

In this study we monitored 13 blazars during 58 nights between the years 2006 and 2011 for a total of about 160 h. Our goal was to establish the general character of the variations on intra-night time-scales. Even though there are a number of reports for very rapid, magnitude-scale ‘frame-to-frame’ variations, our observations indicate mostly slow trends or wobbles that can successfully be fitted with a low-order polynomial (Section 3), and for many objects/nights we found no variations at all.

We continue below with a description of our observational data.

## 2 OBSERVATIONAL DATA

We employed several instruments equipped with CCD cameras and standard *UBVRI* filter sets to perform the photometric monitoring. These include the 60-cm reflector of Belogradchik Observatory, Bulgaria (coded B60 in Table 1), equipped with SBIG ST-8 CCD (as of 2009 replaced with FLI PL9000); the 2-m RCC reflector (Photometrics AT200 CCD) and the 50/70-cm Schmidt camera (SBIG ST-8, later replaced with FLI PL16803 CCD) of Rozhen National Observatory, Bulgaria (coded R50/70 and R200 respectively); and the 104-cm reflector of ARIES, Nainital, India (Wright 2k CCD), coded as A104. Further details on the instruments used can be found in Gaur et al. (2012b).

A total of almost 3000 individual frames were obtained and analysed.<sup>2</sup> The typical exposure time was 120 s; however, depending on the brightness of the object and the telescope size, different exposure times between 60 and 240 s were used on different occasions. The monitoring was performed mostly in the *R* band with a few exceptions, for which the *I* band or no filter was used (Table 1). The latter was the case for two very weak objects, monitored with a relatively small telescope; see Bachev, Strigachev & Semkov (2005) for comments on this issue. The majority of the nights were clear and stable, but on a few occasions we monitored during unfavourable atmospheric conditions, which resulted in larger and variable photometric errors (see Section 4.1 for a discussion).

After bias, dark-current (where appropriate) and flat-field corrections, the magnitudes were extracted by applying standard-aperture photometry routines. The aperture radius was taken to be typically 2–3 times the seeing. The magnitudes of the blazar and a check star were measured with respect to a main standard of known magnitude, with no further corrections made. Both the main standard and the check star were chosen on the basis of their magnitude, colour and spatial proximity to the blazar; however, owing to the different instrumental characteristics (fields of view), no formal criteria were applied.

Table 1 gives a short log of the observations. The columns give the object name, the UT date when the observation started, the instrument, the monitoring duration in hours, the number of observational points for the corresponding run, and the filter. An asterisk

**Table 1.** Observations.

Object	UT date	Telescope	Duration	Points	Filter
3C 66A (0219+428)	14.10.2007	R50/70	1.1	18	R
	02.11.2007	B60	2.8	79	R
	03.11.2007	B60	1.9	53	R
	08.10.2009	A104	1.6	31	R
1ES 0229+200	09.10.2009	A104	5.3	67	R
	21.11.2009	A104	4.4	48	R
AO 0235+16	20.02.2007	R50/70	0.9	20	R
	25.02.2007	R50/70	1.0	20	R
4C 47.08 (0300+470)	10.10.2009	A104	3.8	49	R
	22.11.2009	A104	1.1	13	R
S5 0716+714	16.01.2007	B60	1.3	19	R
	18.01.2007	B60	0.9	19	R
	24.02.2009	B60	6.6	161	I
	25.02.2009	B60	6.4	180	I
PKS 0735+178	08.10.2009	A104	1.6	32	R
	20.12.2009	A104	6.9	115	R
PKS 0736+017	29.02.2008	B60	5.5	77	NO
	03.03.2008	B60	3.5	40	NO
	25.01.2011	B60	3.3	44	NO
	25.04.2011	B60	0.8	21	NO
OJ 287 (0851+202)	19.11.2006*	B60	0.9	26	R
	14.12.2006	R200	4.2	98	R
	17.12.2006*	R50/70	1.9	30	R
	20.02.2007*	R50/70	1.9	30	R
	08.04.2007*	R200	1.8	40	R
	09.04.2007	R200	2.1	50	R
	10.04.2007*	R50/70	2.9	45	R
29.02.2008*	R50/70	2.8	75	R	
3C 279 (1253-055)	26.01.2006	B60	0.5	15	R
	27.01.2006	B60	1.1	30	R
	28.01.2006	B60	0.7	20	R
3C 345	20.06.2007	R200	3.4	69	R
BL Lac (2200+420)	15.07.2007*	R200	0.4	10	R
	16.07.2007	R200	3.1	47	R
	14.08.2007	R200	1.9	50	R
	15.08.2007	R200	2.7	70	R
	16.08.2007	R200	2.3	75	R
	18.08.2007	R50/70	3.4	70	R
	19.08.2007	R50/70	3.2	58	R
	20.08.2007	R50/70	3.0	55	R
	02.11.2007	B60	0.7	20	R
	07.12.2007*	B60	2.0	47	R
08.01.2008	B60	2.6	61	R	
09.01.2008*	B60	2.3	58	R	
11.01.2008	B60	1.8	49	R	
07.07.2008	R200	1.5	74	R	
08.10.2009	A104	4.0	78	R	
3C 454.3 (2251+158)	28.07.2008	B60	1.9	54	R
	29.07.2008	B60	2.2	62	R
	30.07.2008*	B60	2.2	63	R
	31.10.2010*	R50/70	5.0	27	R
	01.11.2010*	R50/70	5.8	27	R
	02.11.2010*	R50/70	5.3	30	R
	03.11.2010*	B60	6.7	57	R
04.11.2010*	B60	3.1	29	R	
06.11.2010*	R50/70	3.6	21	R	
B2 2308+341	10.08.2010	B60	2.8	40	NO
	11.08.2010	B60	2.1	30	NO

<sup>1</sup> Details at <http://www.to.astro.it/blazars/WEBT>.

<sup>2</sup> Some of these data may also have been used in active WEBT campaigns.

after the date indicates an observation used for the statistics but not shown in the figures.

### 3 RESULTS

Figs 1–8 show the results of our intra-night variability study. The top panel of each box shows the blazar light curve (LC), and the bottom one shows the check star LC, both measured with respect to the main standard. The object name and the UT date are given at the top of each box.

#### 3.1 The nature of the intra-night variations

As can be seen from Figs 1–8, the blazar LCs can be described as smooth fluctuations or trends without any violent, ‘frame-to-frame’ changes. Furthermore, no statistically significant variations are present at all on many occasions. Therefore, it would be appropriate to fit the LCs with a straight line or – less often ( $\sim 40$  per cent of the cases) – with a low-order polynomial. This approach enables us to better represent the variations and to eliminate to a

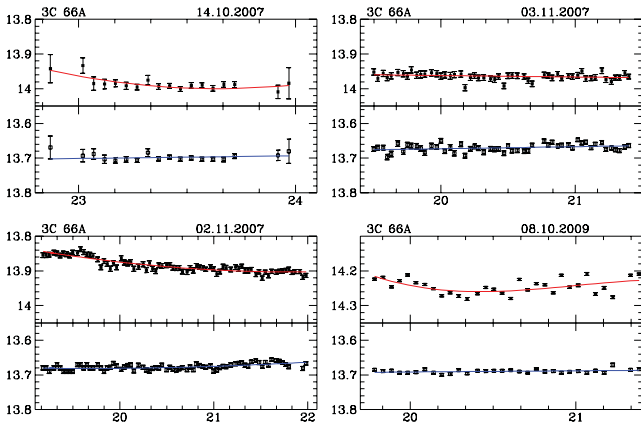


**Figure 1.** Intra-night blazar light curves (LCs; 3C 66A data). The upper panel of each box shows the blazar LC (filled symbols), measured with respect to a main standard, and the lower one shows the same for a check star (open symbols). The photometric errors at the  $1\sigma$  level are indicated as error bars. The best-fitting low-level polynomial (see the text) is also shown for both the blazar and the check star LCs. The name of each monitored object and the UT date when the observation started are shown at the top of each box. The abscissa shows the UT in hours. Each upper panel has the same vertical scale factor as the corresponding lower panel, but the exact value may differ from object to object.

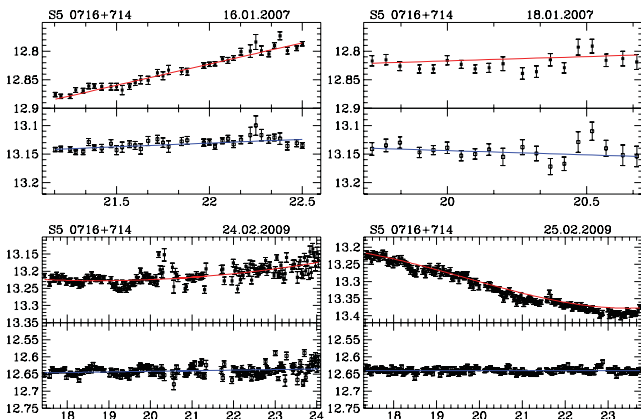


**Figure 2.** As Fig. 1, but for S5 0716+714.

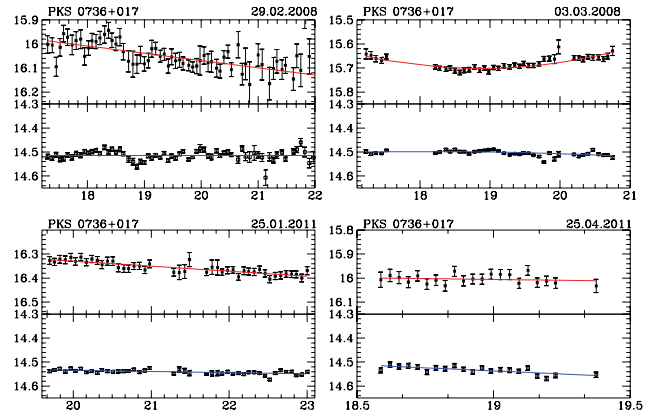


**Figure 3.** As Fig. 1, but for PKS 0736+017.

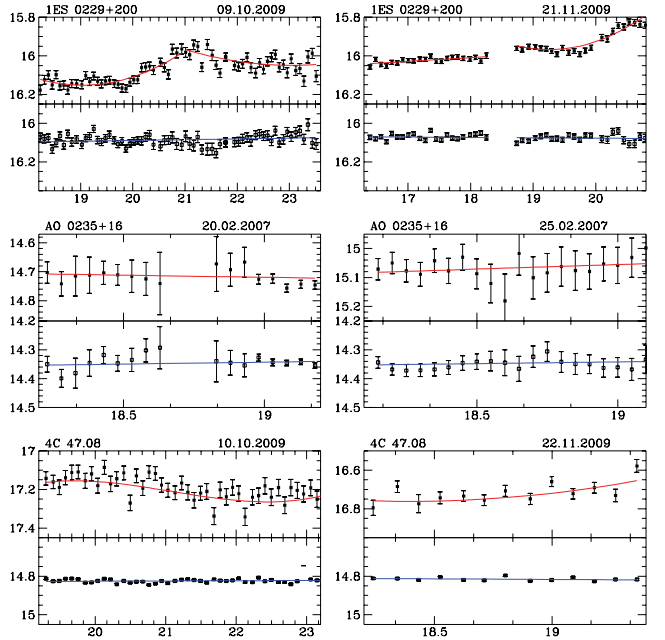


**Figure 4.** As Fig. 1, but for 1ES 0229+200, AO 0235+16 and 4C 47.08.

large extent any spurious effects introduced by the photometric errors. The fitting of a low-order polynomial was successfully applied by Bachev et al. (2011) to search for time delays between different optical bands (see also Montagni et al. 2006, who used straight lines to fit different segments of the LCs). The corresponding best fits are also shown in Figs 1–8 for the LCs of both blazars and check stars. As can be seen, the fits are quite successful in most (but perhaps not all!) cases, even though some of the runs lasted for more than 5 h. Fitting LCs allows the distribution of magnitude change rates,  $dm/dt$ , to be studied for all objects individually, as well as for the entire sample (Section 3.3).

The order of the polynomial was chosen to be as low as possible, and a linear slope was used in almost 50 per cent of cases. Unfortunately, there is no easy way to use statistics (e.g.  $\chi^2$ ) to determine the degree of the polynomial. The reason is that the real photometric errors are often larger (e.g. Bachev et al. 2005 and references therein) than the theoretical ones by a factor that is difficult to determine and may well vary from instrument to instrument and/or with observing conditions. Furthermore, correcting the theoretical errors by a certain factor does not seem to be good practice (de Diego 2010). We note, though, that the distributions of the

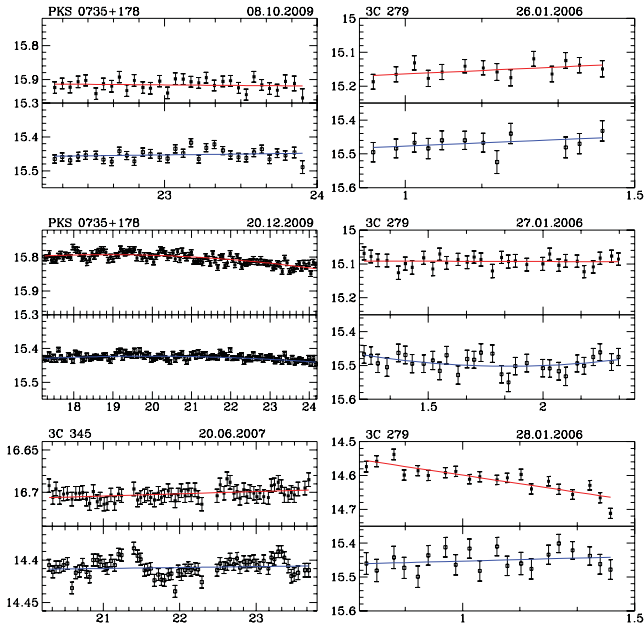


**Figure 5.** As Fig. 1, but for PKS 0735+178, 3C 279 and 3C 345.

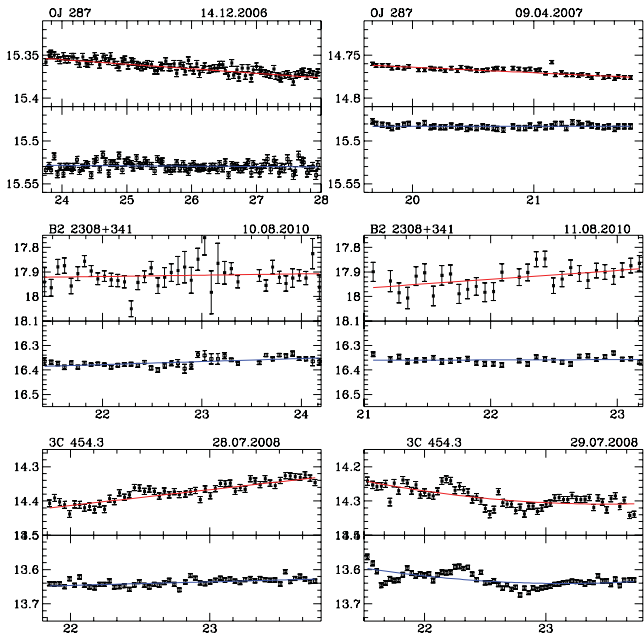


**Figure 6.** As Fig. 1, but for OJ 287, B2 2308+341 and 3C 454.3. For OJ 287 only two out of eight LCs are shown. For 3C 454.3, only two out of nine LCs are shown; see Bachev et al. (2011) for the rest of them.

magnitude change rates depend very little on the exact polynomial order, as long as this order is kept much lower than the number of data points.

Even though we find no rapid variations (say more than a few hundredths of a magnitude on a minute time-scale), there are sometimes such claims in the literature, some of which concern objects from our sample. It is difficult to judge the veracity of these results as often there is no independent way to verify them. See Cellone et al. (2007) for examples and a critical analysis.

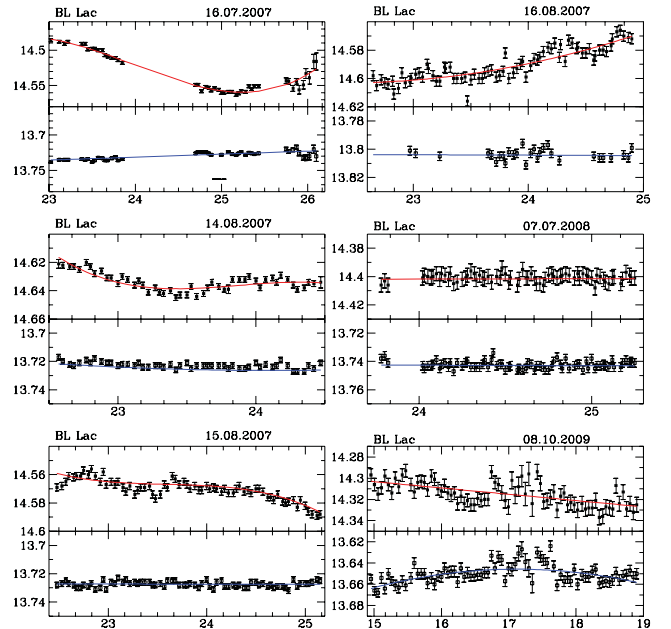


**Figure 7.** As Fig. 1, but for BL Lac. Larger-telescope data, six out of seven nights shown.

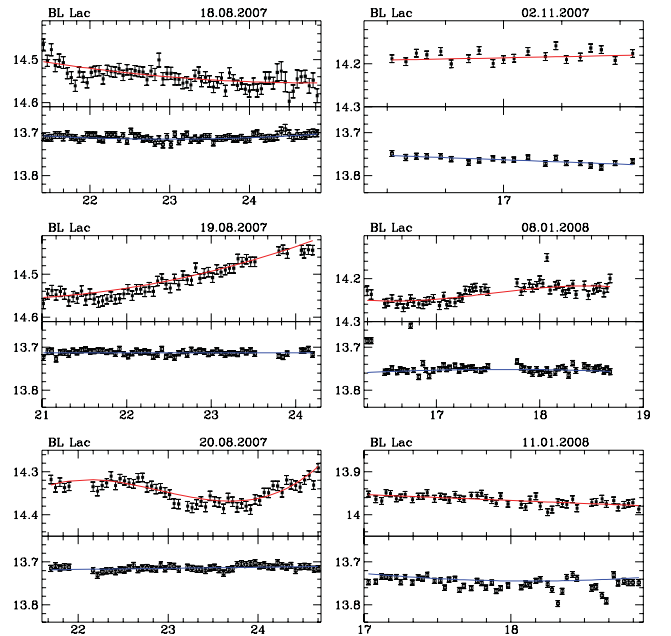


**Figure 8.** As Fig. 1, but for BL Lac. Smaller-telescope data, six out of eight LCs shown.

### 3.2 Individual notes

**3C 66A.** During four nights of monitoring (Fig. 1), this TeV blazar showed only minor ( $\sim 0.05 \text{ mag h}^{-1}$ ) variations at best. This behaviour is consistent with the reports by Raiteri et al. (1998), Dai et al. (2001), Sagar et al. (2004), Böttcher et al. (2009) and Rani et al. (2011b), wherein 3C 66A was observed at a similar brightness stage and showed similar short-term variability. Although a rapid change was reported on one occasion ( $\Delta B \simeq 0.5 \text{ mag h}^{-1}$ ; Zhang et al. 2004), overall the object does not seem to be highly active most of the time, showing only minor, smooth variations.

**1ES 0229+200.** We monitored this very high-energy  $\gamma$ -ray source for two nights for a total of  $\sim 10$  h (Fig. 4). To the best of our knowledge, no results of previous intra-night optical monitoring of this object have been published, and Kurtanidze et al. (2004) found no variations on longer time-scales. Our monitoring, however, indicates the presence of rapid intra-night variability of up to  $0.15 \text{ mag h}^{-1}$ . As a matter of fact, this is one of the few objects for which even a third-degree polynomial did not seem to fit the LC very well. For this particular object we had to use two different polynomials to fit the entire LC.

**AO 0235+164.** We monitored this object as part of an active WEBT campaign (Raiteri et al. 2008a) during two photometrically poor nights (Fig. 4) and found practically no intra-night variations; however, a change of  $\Delta R \simeq 0.4$  mag was seen within  $\sim 5$  days. Other authors (Hagen-Thorn et al. 2008), though, report significant intra-night variations of  $\Delta R \simeq 0.5$  mag within several hours. Romero et al. (2000, 2002) also observed rapid changes, indicating that variations of  $\Delta R \simeq 0.1 \text{ mag h}^{-1}$  may be typical for this otherwise highly active object (see also Sagar et al. 2004; Gupta et al. 2008; Rani et al. 2011b).

**4C 47.08.** This *Fermi*-LAT source (Abdo et al. 2010) has rarely been studied at optical wavelengths. We found a  $\sim 0.5$ -mag variation on the time-scale of a month, but only minor variations during the two nights of intra-night monitoring. The object was weak, and the photometric uncertainties might have contributed to the apparent variations, seen as smooth fluctuations (Fig. 4). We note that Star C5 (the closest standard, Fiorucci et al. 1998) appears to be variable on short time-scales.

**S5 0716+714.** This blazar has been a target of a number of intra-night monitoring campaigns. Practically all studies, for example Sagar, Gopal-Krishna & Mohan (1999), Nesci, Massaro & Montagnani (2002), Wu et al. (2005), Gu et al. (2006), Montagnani et al. (2006), Pollock, Webb & Azarnia (2007), Gupta et al. (2008), Stalin et al. (2009), Poon, Fan & Fu (2009), Carini, Walters & Hopper (2011) and Rani et al. (2011b), report significant variations, which can typically be described as smooth fluctuations or a sequence of trends, often abruptly changing direction. Some reports even imply the presence of very rapid (tenths of a magnitude) changes within a few minutes (Fan et al. 2011) and/or quasi-periodic oscillations (Gupta, Srivastava & Wiita 2009; Rani et al. 2010) on a  $\sim 15$ -min time-scale. Clearly, S5 0716+714 is one of the most active blazars in terms of rapid intra-night variations. Our monitoring during four nights showed smooth trends, reaching up to  $\sim 0.05 \text{ mag h}^{-1}$ , but no rapid changes on a minute time-scale (Fig. 2)

**PKS 0735+178.** This is another object that has been extensively studied in optical wavelengths over the years. Some of the more recent studies by Bai et al. (1999), Sagar et al. (2004), Stalin et al. (2004), Gupta et al. (2008), Goyal et al. (2009) and Rani et al. (2011b) report only low-level intra-night variations, if any at all. On the other hand, Zhang et al. (2004) found variability of  $\sim 0.5 \text{ mag h}^{-1}$  on one occasion. Our observations confirm what most the researchers report; that is, we found practically no variability during two nights for a total of about 8.5 h of monitoring (Fig. 5).

**PKS 0736+017.** This flat spectrum radio quasar (FSRQ) is known to show occasionally exceptional variability on intra-night scales. Clements, Jenks & Torres (2003), for instance, reported a 1.3-mag outburst within 2 h. Their observations, however, as well as our results imply that PKS 0736+017 is much more active when close to its maximum ( $R \simeq 13.7$  mag), or at least that periods of intra-night activity are followed by periods of almost constant brightness. Sagar

et al. (2004) also reported very quiescent behaviour when the object was around  $R \simeq 15$  mag. Our observations (Fig. 3) were during a deep minimum, of  $\sim 16$  mag (see also Ramírez et al. 2004), but some low-level, smooth variations are seen.

**OJ 287.** This object manifested very little if any intra-night variability during eight nights of monitoring spanning  $\sim 15$  months, although night-to-night variations of  $\sim 0.1$  mag were present. In Fig. 6 we only show the results from two atmospherically stable nights, where gradual trends are clearly seen. In spite of the fact that we found no rapid variations during our monitoring of this object, other authors report significant changes on very short time-scales. Zhang et al. (2007), for instance, found a  $\Delta R \simeq 0.35$ -mag change for half an hour during one night (see also Xie et al. 2001). On the other hand, Carini et al. (1992), González-Pérez, Kidger & de Diego (1996), Dultzin-Hacyan et al. (1997), Sagar et al. (2004), Gupta et al. (2008) and Rani et al. (2011b) report only minor variations, if any, which is much more consistent with our findings.

**3C 279.** This object was monitored on three consecutive nights in 2006 January, when it was around 15 mag (much fainter than its historical maximum,  $R \simeq 12.5$  mag). A clear decreasing trend of  $0.15 \text{ mag h}^{-1}$ , probably tracing the end of a small outburst (Fig. 5; see also Böttcher et al. 2007, for a long-term LC covering this period), was seen on one night, while during the other two nights the object was rather stable. Kartaltepe & Balonek (2007) reported similar gradual trends (if any) during their monitoring, when the object was around 14 mag. Gupta et al. (2008) found practically no variability during their monitoring, but, in contrast, rapid changes were reported by Miller et al. (2011) for the low brightness state. Clearly, 3C 279 exhibits different types of intra-night variability behaviour.

**3C 345.** This superluminal FSRQ has not been observed for intra-night variability very often, probably because it has been weak ( $\sim 16$ – $17$  mag) in recent years. Mihov et al. (2008) and Howard et al. (2004) found practically no intra-night variability. In contrast, Wu et al. (2011a) reported trends of  $\sim 0.2 \text{ mag h}^{-1}$ , while Kidger & de Diego (1990) found an even sharper decline on one occasion. We monitored this object over one night and found no variations at all (Fig. 5).

**BL Lac.** We monitored the blazar archetype extensively for a total of almost 35 h during 15 nights, on six of which a 2-m-class telescope was used (Figs 7, 8). Variability pictures reveal trends of up to  $\sim 0.1 \text{ mag h}^{-1}$  or smooth fluctuations. The object was mostly around  $R \sim 14.5$  mag, meaning a rather low state, and showed little night-to-night variability (Raiteri et al. 2009). Other researchers report similar intra-night behaviour (Nesci et al. 1998; Speziali & Natali 1998; Papadakis et al. 2003; Howard et al. 2004), for example smooth variations of typically  $\sim 0.1 \text{ mag h}^{-1}$ . However, Zhang et al. (2004) found unusual  $\simeq 0.3$ -mag frame-to-frame variations.

**3C 454.3** This is another well-studied FSRQ. Some of the recent intra-night variability studies include those of Poggiani (2006), Gupta et al. (2008), Rani et al. (2011b) and Gaur, Gupta & Wiita (2012a), who found only minor or no variations, but variability rates of  $\sim 0.2 \text{ mag h}^{-1}$  were seen occasionally. A similar behaviour (see also Fig. 6) was also reported by Bachev et al. (2011), who monitored the object during a recent outburst to search for time delays between different optical bands on intra-night time-scales. Their *R*-band LCs were also used for the purposes of this work. Zhai, Zheng & Wei (2011) performed a similar search but neither of these works found convincing evidence for a delay between the optical bands. Raiteri et al. (2008b), on the other hand, give clear examples of

violent intra-night variability episodes of  $\sim 1 \text{ mag h}^{-1}$ , perhaps tracing short-lasting outbursts during the high-activity phase of the blazar. Obviously, this object demonstrates different variability behaviour, probably depending on its brightness state.

**B2 2308+341** Optical monitoring of this object was triggered by increased  $\gamma$ -ray activity (D’Ammando 2010). The object was very weak, so no filter was used during the two nights of monitoring. Thus, the magnitudes shown in Fig. 6 are somewhat arbitrary. No huge intra-night or day-to-day variations were observed. The object has rarely been studied, and we found no other works on intra-night variability.

### 3.3 Distribution of the variability rates of the sample

The LCs we analyse in this work cover a total of  $\sim 160 \text{ h}$  of monitoring. Although the LC data cannot be considered complete, and the sample cannot be considered representative, it still may be worthwhile to build a histogram of the magnitude change rates ( $dm/dt$ ) for the entire sample. Such a histogram may be helpful in the study of time asymmetries, for instance. Fig. 9 shows the distribution of  $dm/dt$  values for the blazars (upper panel) and the check stars (lower panel) based on the corresponding best fits. Normally, one would not expect the check stars to show variations; however, sometimes slow trends became evident after applying the same fitting procedure as for the blazars, resulting in some non-zero values in the  $dm/dt$  histogram for the check stars. Explanations can be sought in terms of variable atmospheric conditions, possible low-level stellar variability, etc. (see Klimek et al. 2004; Bachev et al. 2005), but this goes beyond the scope of this paper.

There are two important results that are worth mentioning. First, it seems that observations of significant variability rates are very rare. For instance, from Fig. 9 we find only a  $\sim 2$  per cent chance of observing blazar variability  $|dm/dt| > 0.1 \text{ mag h}^{-1}$  and a  $\sim 25$  per cent

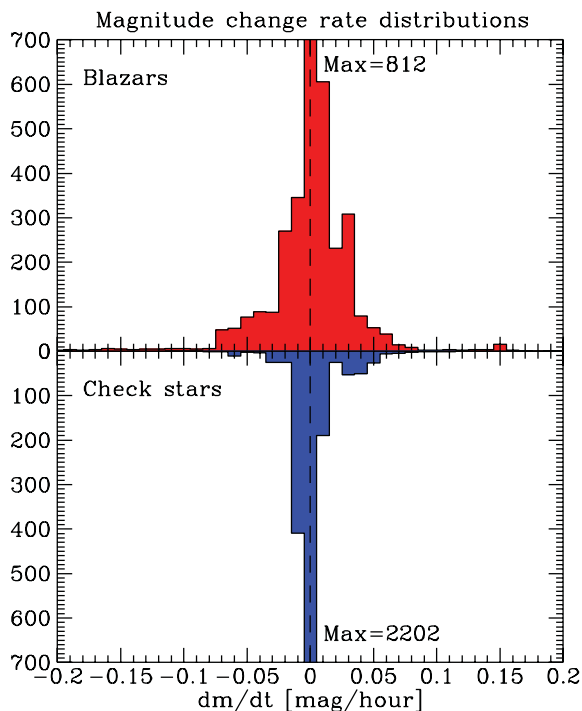


**Figure 9.** Magnitude change rates for the blazars and the check stars, as found from the fitting polynomials. The numbers in the distribution count the 3-min intervals from the LC with the corresponding magnitude change rate.

chance of observing practically no detectable variability,  $|dm/dt| < 0.005 \text{ mag h}^{-1}$  (the corresponding percentage for the check stars is  $\sim 68$ ). Second, the distribution does not appear to be symmetric. Statistical tests to compare the means, medians and standard deviations, as well as the Kolmogorov–Smirnov test, performed separately on the ‘negative’ and ‘positive’ parts of the  $dm/dt$  distribution distinguish them at the 99.9 per cent level, even though the mean of the entire distribution is consistent with zero within the errors (as expected). This might be a result of the data incompleteness; however, it might also be an artefact of a real time asymmetry of the blazar LCs. Because the total monitoring times were very different for different objects, we cannot claim that such asymmetry, if real at all, is a general property of the sample or, to an even lesser extent, of the entire blazar population.

### 3.4 Possible quasi-periodic oscillations

Employing a 2-m-class telescope to monitor some of the objects (BL Lac in particular) ensured photometry of very high accuracy (e.g. 0.002–0.003 mag) during some stable nights, which allowed possible (quasi-periodic) micro-oscillations to be studied. Such micro-oscillations have been previously reported; for example Clements et al. (2003) for PKS 0736+017; Wagner et al. (1996), Gupta et al. (2009) and Rani et al (2010) for S5 0716+714. For BL Lac, some hints of quasi-periodicity were presented by Speziali & Natali (1998, their fig. 3), although the authors do not claim any statistical significance. It is clear from our BL Lac data (the most extensively studied object in our sample) that a periodic signal is not the dominant feature in the LCs. However, after subtracting the leading polynomial, one can attempt to search for micro-oscillations in the residuals. We found some clues for the presence of such micro-oscillations with an amplitude of  $\leq 0.01 \text{ mag}$  and a typical period  $T \sim 1 \text{ h}$  for many of the nights (Fig. 10).

Interestingly, the oscillation pattern does not appear to depend much on the order of the leading polynomial (within some limits, of course) used to fit the LC. If confirmed, micro-oscillations with a period of an hour or so may have significant implications for our understanding of how matter accelerates along the jet. We note, however, that such a period is close to the shortest possible *Keplerian* time (perhaps even below the innermost stable orbit, Section 4.3).

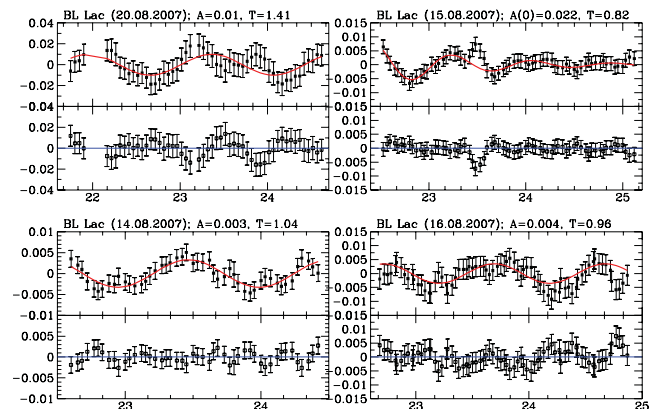


**Figure 10.** BL Lac light curves after subtracting the leading polynomial (Fig. 7). A moving-average filter is applied to the data to reduce the scatter. Micro-oscillations are clearly seen on some nights (e.g. 14.08.2007). The upper panels show the sine function best fits, and the lower ones show the residuals. For the night of 15.08.2007, an exponentially decaying sine amplitude works best.

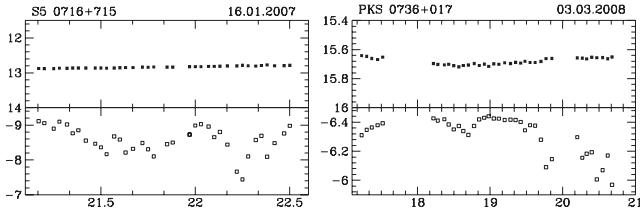


**Figure 11.** The influence of atmospheric transparency on the differential light curves of the blazars S5 0716+714 and PKS 0736+017 monitored during two unstable nights. The upper boxes show the blazar LCs, and the lower ones show the signal from the main standard, transformed into arbitrary magnitudes. It can be seen that the atmospheric stability does not have any visible effect on the differential LCs.

## 4 DISCUSSION

### 4.1 Differential light curves and atmospheric stability

Because the colours of the blazars and the stars used for the differential photometry may sometimes differ significantly, the influence of the atmospheric stability and/or air-mass change on the differential LCs should be considered. In order to check for any effects we consider closely cases when the blazar showed significant variations during the monitoring on unstable nights. Fig. 11 shows two such cases. The upper boxes show the blazar LCs, and the lower ones show the signal from the main standard, transformed into arbitrary magnitudes. It can be seen that, while the magnitude of the main standard varied significantly, because of both the changing air mass and the unstable atmosphere, the differential blazar LCs do not seem to be influenced at all, which leads to the conclusion that the observed trends are unlikely to be attributable to the changing atmospheric transparency. The Pearson correlation coefficients between the two data sets are  $-0.36$  for S5 0716+714 and  $-0.66$  for PKS 0736+017, implying an insignificant correlation. Spearman rank correlation coefficients are even less significant, namely  $-0.27$  and  $-0.41$ , respectively. As a matter of fact, a small anticorrelation between the data sets is actually expected, as the photometric errors of the main standard influence both data sets.

### 4.2 Implications of the variability models

#### 4.2.1 Time asymmetry of the light curves

Studying the distribution of the magnitude gradients may help to disentangle the different variability scenarios. For instance, a dissipative process (i.e. an explosive event, etc.), being by nature not time-reversible, will probably produce a time-asymmetric LC (perhaps with sharp rises and slow declines), which will result in different positive and negative magnitude change rate distributions. On the other hand, a process described by a conservative dynamical system, whose Hamiltonian is not directly dependent on time<sup>3</sup> (such as microlensing, orbital motion, etc.), will probably produce a time-symmetric LC, leading to a symmetric positive/negative gradient distribution. Unfortunately, our data (Fig. 9) cannot be considered statistically significant (Section 3.3) for a firm conclusion for a number of reasons.

<sup>3</sup> For more details see, for example, Lamb & Roberts (1998) and references therein.

#### 4.2.2 Evolution of the electron energy density distribution

A natural cause of the brightness changes could be the evolution of the energy density distribution of the relativistic particles,  $n(\gamma)$ , which leads to a variable synchrotron emission. While the energy loss rates are known (both synchrotron and Compton losses are  $\propto \gamma^2$ , where  $\gamma$  is the electron's Lorentz factor; Rybicki & Lightman 1979), the energy gain rates (the acceleration/injection mechanisms) are generally unknown. This leads to the impossibility of solving the corresponding *Fokker-Planck* equation (Rybicki & Lightman 1979) without a priori imposed assumptions. Electron energy density evolution will probably lead to time delays between different wavebands (Bachev et al. 2011 and references therein). Knowing that our LCs are monochromatic, and taking into account the above, means that testing this variability mechanism is beyond the scope of this study.

#### 4.2.3 Swinging jet

The idea behind this variability mechanism is that the path of the relativistically moving blobs along the jet can deviate slightly from a straight line, leading to a variable Doppler factor and thus to variable emission from that particular blob (Fig. 12 illustrates the situation; see also Gopal-Krishna & Wiita 1992). The definition of the Doppler factor is  $\delta \equiv 1/\Gamma(1 - \beta \cos \theta) = 1/\Gamma(1 - \beta \mu_0 \cos \varphi)$ , where  $\mu_0 = \cos \theta_0$  and  $\theta_0$  is the ‘impact parameter’, that is, the smallest angle between the jet direction (direction of motion of the blob) and the line of sight. Clearly, the maximum amplification occurs when  $\theta_0 = 0$ .

If we take into account that all angles are small (we consider only cases where the magnification is significant), it can be shown that  $\delta = A/[1 + (t/\tau)^2]$ , where  $A$  is a constant and  $\tau$  is a characteristic time-scale.

The associated magnitude change (if this blob is dominating the blazar emission at some particular moment) can be calculated taking into account that the flux  $F_\nu = F_{\nu'} \delta^{3+\alpha}$ , where  $\alpha$  is the spectral index i.e.,  $F_\nu \propto \nu^{-\alpha}$ . Thus,  $dm/dt \simeq d \ln \delta / dt$  (see also Nesci et al. 2002;

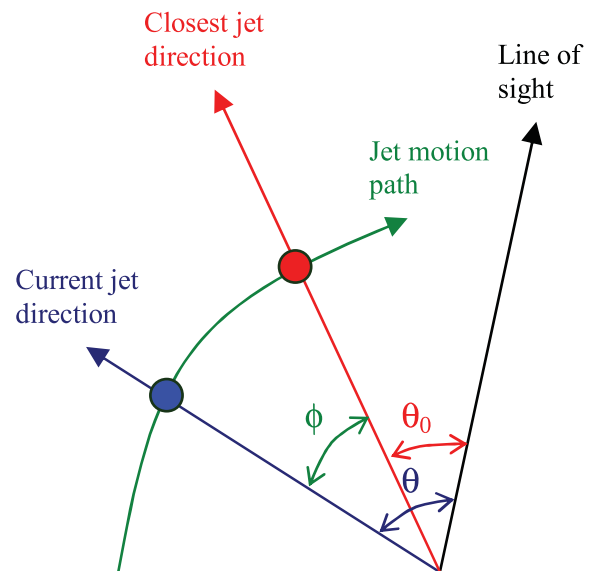


**Figure 12.** Sketch showing the change of the jet direction and the corresponding angles (see text).

Montagni et al. 2006). Knowing  $dm/dt$ , one can integrate to obtain the magnitude of the blob emission as a function of time.

As expected,  $m(t)$  is in general a complex peak function, but for practical purposes it can be approximated with a simpler one. For  $t \gg \tau$ , the peak appears quite sharp, and the best working simple function here is the exponent. However, the magnitude change becomes significant, for example  $\sim 10$  mag (see also Gopal-Krishna & Wiita 1992). Because such large amplitudes are never observed in the blazar LCs, it has to be assumed that a flare from a single blob, owing to a variable Doppler factor, may never completely dominate the blazar emission, except perhaps for  $t \leq \tau$ . Thus, a correct approach would be to invoke an additional constant-flux component of magnitude  $m_1$ , which can be the result of host galaxy emission and/or of an ensemble of independent flaring events, each at a different evolutionary state (but most of them far from the maximum).

Introducing the constant component changes significantly the shape of the flares; this time the best working fit appears to be a *Gaussian* for a fairly broad range of ratios between  $m$  and  $m_1$ . In other words, unless we accept that a flare can be so powerful as to increase the total blazar emission by many orders (say by more than 10 mag), its overall shape has to resemble a Gaussian within the framework of this model.

#### 4.2.4 Microlensing

We can use a similar scheme to compute the LC of an emitting blob whose emission is magnified as a result of microlensing from a star (a point-mass lens) along the line of sight (Paczynski 1996). The flux magnification for gravitational lensing is  $M = [\hat{\theta}^2 + 2]/\hat{\theta} \sqrt{\hat{\theta}^2 + 4}$ , where  $\hat{\theta} = \theta/\theta_E$ , where  $\theta$  is the Einstein radius (see for instance Narayan & Bartelmann 1996, for a review).

Under the appropriate assumptions one can calculate  $M(t)$  and in turn the LC if the emission is dominated by a single, microlensed blob. In this case the best working fit appears to be the *Lorentzian*, gradually being transformed into an exponent for strong microlensing events; see also Paczynski (1996). Interestingly, adding a constant flux as before does not seem to affect significantly the shape of the flare (within some limits).

#### 4.2.5 Comparison with observations

A dense LC covering a relatively long time interval may allow the shapes of the individual flares to be studied and thus help to constrain the models. As we saw, the last two models we considered in detail predict in general different flare shapes, which is especially true for the stronger flares.

On the other hand, a number of authors have successfully modelled the blazar flares with exponents (Valtaoja et al. 1999; Böttcher & Príncipe 2009; Hovatta et al. 2009; Chatterjee et al. 2012), which resembles the case of a strong microlensing event.<sup>4</sup> Most of these authors, however, used different rising and decaying times for their exponential fits, which cannot be easily explained in terms of microlensing (see also Reithal et al. 2012, statistics on time-asymmetry for many objects). If not attributed to a possible degeneracy of the fitting procedure when applied to multiple flares, such a time asymmetry might be a result of the evolution of the electron energy density distribution; that is, of different characteristic times of

the acceleration and energy-loss mechanisms. Having said that, we stress again that to calculate the emission it is necessary to solve the *Fokker–Planck* equation. For example, even if the energy loss were the only mechanism to modify the energy density distribution of the relativistic particles, this would not necessarily mean a decreasing flux at certain wavelengths and vice versa.<sup>5</sup> Actually, the asymmetric flares can also result from jet inhomogeneity with a combination of jet curvature (e.g. Villata et al. 2009).

Unfortunately, during our monitoring we could not trace individual flares, so it is difficult to distinguish which one (if any) of the models is most important for producing the variability (the flares) or even which one plays the most important role. The situation becomes even more complicated if one considers a combination of different flares with different phases and amplitudes to produce the observed variability picture. In any case, the presence of very sharp peaks seems to favour microlensing. It is also possible that different mechanisms govern the flux changes at different time-scales.

### 4.3 Radiation from the black hole vicinity?

Possible quasi-periodic oscillations with a period of an hour or so (the BL Lac case, Fig. 10), if associated with Keplerian motion around the supermassive black hole, may impose certain constraints on the black hole characteristics – the mass ( $M_{\text{BH}}$ ) and the spin parameter ( $a$ ). The Keplerian period (in hours) at a distance  $r$  is  $t_K \simeq (r^{3/2} + a)M_8$ , where  $M_8$  is the central mass in  $10^8$  solar masses (e.g. Shapiro & Teukolsky 1983), and  $r$  is in units of  $M$  (geometrical units used,  $G = c = 1$ ). Because the horizon is determined by  $r_{\text{H}} = 1 + (1 - a^2)^{1/2}$ , one obtains (taking that  $t_K \simeq 1$ )  $M_8 \leq 0.5$  for any value of the black hole spin ( $0 \leq a \leq 1$ ). The mass should be even smaller if one accepts a much more physical assumption, namely that the oscillation results from some instabilities at the innermost stable circular orbit ( $r_{\text{ISCO}}$ ), instead of at the horizon. The last distance depends in a complex way on the spin and the mass (e.g. Shapiro & Teukolsky 1983). A simple useful fit for practical purposes that works well everywhere, except for  $a \simeq 1$ , and combines  $t_K$  (in hours) at  $r_{\text{ISCO}}$  with the black hole parameters, is the following expression:  $M_8 \simeq t_K/\sqrt{330.7 e^{-a} - 115.2}$ . Therefore,  $M_{\text{BH}}$  should be between  $7 \times 10^6 M_{\odot}$  for  $a = 0$  and  $4 \times 10^7 M_{\odot}$  for  $a = 0.998$  (Fig. 13) if the oscillations are the result of Keplerian motion at  $r_{\text{ISCO}}$ . Such a mass is at least an order of magnitude lower than what the host galaxy magnitude suggests for BL Lac (Wu, Liu & Zhang 2002; Falomo, Carangelo & Treves 2003), but is similar to other estimates, based on the variability characteristics (Xie et al. 2002). It is clear that because the link between these possible quasi-periodic oscillations and the orbital motion is far from proven, no firm conclusion is possible at this stage. Studying such oscillations, however, if further confirmed with high-accuracy observations, could become one of the very few ways to probe the innermost regions of blazars.

## 5 CONCLUSIONS

We publish the optical intra-night LCs of 13 blazars (BL Lacs and FSRQs), covering a total of  $\sim 160$  h of monitoring time. In the majority of cases we detected no variability at all, and when variations were found, they resembled mostly linear trends or smooth fluctuations. In any case, we observed no erratic, ‘frame-to-frame’ changes, which are sometimes reported. The smoothness of the LCs

<sup>4</sup> One should bear in mind, however, that many of these authors used flux units, not magnitudes, when fitting the flares.

<sup>5</sup> If attributable to energy loss, the synchrotron flux will drop at all wavelengths only if  $\alpha > 2$ , where  $n(\gamma) \propto \gamma^{-\alpha}$ .



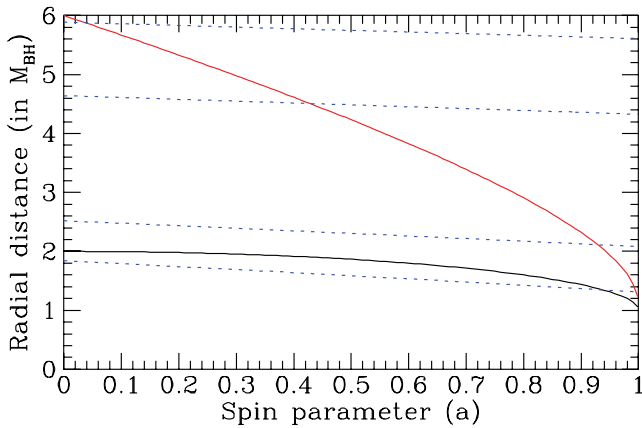


**Figure 13.** The radial distances for an orbital period of 1 h as functions of black hole mass and spin parameter. Thick continuous lines indicate the innermost stable orbit and the horizon, and dashed lines indicate the 1-h period distances for  $M_8 = 0.07, 0.1, 0.25$  and  $0.4$ , from top to bottom, respectively. Note that all the solutions passing below the horizon line are unphysical there.

allowed fitting of a low-order polynomial, which helped to better reveal the magnitude trends.

The distribution of the magnitude change rates appears to be time-asymmetric, which, if real, would mostly favour models based on electron energy density evolution rather than ‘time-symmetric’ models such as jet swinging or microlensing.

We found some indications for the presence of quasi-periodic micro-oscillations with a period of about an hour in the high-accuracy LCs of BL Lac after subtracting a leading polynomial.

Unfortunately, at this stage we are unable to establish which one of the existing models is most responsible for the blazar variability. It is possible that more than one of them could play some role for the different objects and/or the different activity episodes of a given object. Clearly, further high-accuracy intra-night variability studies are needed for a firm conclusion.

## ACKNOWLEDGMENTS

This research was partially supported by the Scientific Research Fund of the Bulgarian Ministry of Education and Sciences (BIn-13/09 and DO 02-85) and by the Indo-Bulgarian bilateral scientific exchange project INT/Bulgaria/B-5/08 funded by DST, India. We thank the anonymous referee for the rapid response and valuable suggestions. This research made use of CDS-Strasbourg (Simbad) and NASA-IPAC (NED) data bases.

## REFERENCES

Abdo A. A. et al., 2010, *ApJS*, 188, 405  
 Bachev R., Strigachev A., Semkov E., 2005, *MNRAS*, 358, 774  
 Bachev R. et al., 2011, *A&A*, 528, L10  
 Bai J. M., Xie G. Z., Li K. H., Zhang X., Liu W. W., 1999, *A&AS*, 136, 455  
 Böttcher M. et al., 2009, *ApJ*, 694, 174  
 Böttcher M., Principe D., 2009, *ApJ*, 692, 1374  
 Böttcher M. et al., 2007, *ApJ*, 670, 968  
 Carini M. T., Miller H. R., Noble J. C., Goodrich B. D., 1992, *AJ*, 104, 15  
 Carini M. T., Walters R., Hopper L., 2011, *AJ*, 141, 49  
 Cellone S. A., Romero G. E., Araudo A. T., 2007, *MNRAS*, 374, 357  
 Chatterjee R. et al., 2012, *ApJ*, 749, 191

Clements S. D., Jenks A., Torres Y., 2003, *AJ*, 126, 37  
 D’Ammando F., 2010, *The Astronomer’s Telegram*, 2783, 1  
 Dai B. Z., Xie G. Z., Li K. H., Zhou S. B., Liu W. W., Jiang Z. J., 2001, *AJ*, 122, 2901  
 de Diego J. A., 2010, *AJ*, 139, 1269  
 Dultzin-Hacyan D., Takalo L. O., Benítez E., Sillanpää A., Pursimo T., Lehto H., de Diego J. A., 1997, *Revista Mexicana de Astronomía y Astrofísica*, 33, 17  
 Falomo R., Carangelo N., Treves A., 2003, *MNRAS*, 343, 505  
 Fan J.-H., Tao J., Qian B.-C., Liu Y., Yang J.-H., Pi F.-P., Xu W., 2011, *Res. in Astron. and Astrophys.*, 11, 1311  
 Fiorucci M., Tosti G., Rizzi N., 1998, *PASP*, 110, 105  
 Gaur H., Gupta A. C., Wiita P. J., 2012a, *AJ*, 143, 23  
 Gaur H. et al., 2012b, *MNRAS*, 420, 3147  
 González-Pérez J. N., Kidger M. R., de Diego J. A., 1996, *A&A*, 311, 57  
 Gopal-Krishna, Subramanian K., 1991, *Nat*, 349, 766  
 Gopal-Krishna, Wiita P. J., 1992, *A&A*, 259, 109  
 Goyal A. et al., 2009, *MNRAS*, 399, 1622  
 Gu M. F., Lee C.-U., Pak S., Yim H. S., Fletcher A. B., 2006, *A&A*, 450, 39  
 Gupta A. C., Fan J. H., Bai J. M., Wagner S. J., 2008, *AJ*, 135, 1384  
 Gupta A. C., Srivastava A. K., Wiita P. J., 2009, *ApJ*, 690, 216  
 Hagen-Thorn V. A., Larionov V. M., Jorstad S. G., Arkharov A. A., Hagen-Thorn E. I., Efimova N. V., Larionova L. V., Marscher A. P., 2008, *ApJ*, 672, 40  
 Hovatta T., Valtaoja E., Tornikoski M., Lähteenmäki A., 2009, *A&A*, 494, 527  
 Howard E. S., Webb J. R., Pollock J. T., Stencel R. E., 2004, *AJ*, 127, 17  
 Kartaltepe J. S., Balonek T. J., 2007, *AJ*, 133, 2866  
 Kidger M. R., de Diego J. A., 1990, *A&A*, 227, L25  
 Kurtanidze O. M., Nikolashvili M. G., Kapanadze B. Z., Kimeridze G. N., Sigua L. A., Urushadze T. V., Goderidze E. K., 2004, *Nuclear Physics B Proc. Suppl.*, 132, 193  
 Klimek E. S., Gaskell C. M., Hedrick C. H., 2004, *ApJ*, 609, 69  
 Lamb J. S. V., Roberts J. A. G., 1998, *Physica D*, 112, L1  
 Mihov B., Bachev R., Slavcheva-Mihova L., Strigachev A., Semkov E., Petrov G., 2008, *Astron. Nachrichten*, 329, 77  
 Miller H. R., Clemmons H., Maune J. D., Eggen J. R., Gudkova D., Parks J. R., 2011, *arxiv:1104.3887*  
 Montagni F., Maselli A., Massaro E., Nesci R., Sclavi S., Maesano M., 2006, *A&A*, 451, 435  
 Narayan R., Bartelmann M., 1996, *arXiv:astro-ph/96060001*  
 Nesci R., Maesano M., Massaro E., Montagni F., Tosti G., Fiorucci M., 1998, *A&A*, 332, L1  
 Nesci R., Massaro E., Montagni F., 2002, *PASA*, 19, 143  
 Paczynski B., 1996, *ARA&A*, 34, 419  
 Papadakis I. E., Boumris P., Samaritakis V., Papamastorakis J., 2003, *A&A*, 397, 565  
 Poggiani R., 2006, *Ap&SS*, 306, 17  
 Pollock J. T., Webb J. R., Azarnia G., 2007, *ApJ*, 133, 487  
 Poon H., Fan J. H., Fu J. N., 2009, *ApJS*, 185, 511  
 Raiteri C. M., Ghisellini G., Villata M., de Francesco G., Lanteri L., Chiaberge M., Peila A., Antico G., 1998, *A&AS*, 127, 445  
 Raiteri C. M. et al., 2008a, *A&A*, 480, 339  
 Raiteri C. et al., 2008b, *A&A*, 485, L17  
 Raiteri C. M. et al., 2009, *A&A*, 507, 769  
 Ramírez A., de Diego J. A., Dultzin-Hacyan D., González-Pérez J. N., 2004, *A&A*, 421, 83  
 Rani B., Gupta A. C., Joshi U. C., Ganesh S., Wiita P. J., 2010, *ApJ*, 719, 153  
 Rani B. et al., 2011a, *MNRAS*, 417, 1881  
 Rani B., Gupta A. C., Joshi U. C., Ganesh S., Wiita P. J., 2011b, *MNRAS*, 413, 2157  
 Reinthal R. et al., 2012, *J. of Phys.: Conf. Series*, 355, 12  
 Romero G. E., Cellone S. A., Combi J. A., 2000, *A&A*, 360, 47  
 Romero G. E., Cellone S. A., Combi J. A., Andrichow I., 2002, *A&A*, 390, 431  
 Rybicki G. B., Lightman A. P., 1979, *Radiative Processes in Astrophysics*. Wiley Interscience, New York

- Sagar R., Gopal-Krishna, Mohan V., 1999, *A&AS*, 134, 456  
Sagar R., Stalin C. S., Gopal-Krishna, Wiita P. J., 2004, *MNRAS*, 348, 176  
Shapiro S. L., Teukolsky S. A., 1983, *Black Holes, White Dwarfs, and Neutron Stars: The Physics of Compact Objects*. Wiley Interscience, New York  
Speziali R., Natali G., 1998, *A&A*, 339, 382  
Stalin C. S., Gopal-Krishna, Sagar R., Wiita P. J., 2004, *MNRAS*, 350, 175  
Stalin C. S. et al., 2009, *MNRAS*, 399, 1357  
Urry C. M., Padovani P., 1995, *PASP*, 107, 803  
Valtaoja E., Lähteenmäki A., Teräsranta H., Lainela M., 1999, *ApJS*, 120, 95  
Villato M. et al., 2009, *A&A*, 501, 455  
Wagner S. J., Witzel A., 1995, *ARA&A*, 33, 163  
Wagner S. J. et al., 1996, *AJ*, 111, 2187  
Wu X.-B., Liu F. K., Zhang T. Z., 2002, *A&A*, 389, 742  
Wu J., Peng B., Zhou X., Ma J., Jiang Z., Chen J., 2005, *AJ*, 129, 1818  
Wu J., Zhou X., Ma J., Jiang Z., 2011a, *MNRAS*, 418, 1640  
Wu Q., Zou Y.-C., Cao X., Wang D.-X., Chen L., 2011b, *ApJ*, 740, 21  
Xie G. Z., Li K. H., Bai J. M., Dai B. Z., Liu W. W., Zhang X., Xing S. Y., 2001, *ApJ*, 548, 200  
Xie G. Z., Liang E. W., Xie Z. H., Dai B. Z., 2002, *AJ*, 123, 2352  
Zhai M., Zheng W. K., Wei J. Y., 2011, *A&A*, 531, 90  
Zhang X., Zhang L., Zhao G., Xie Z.-H., Wu L., Zheng Y.-G., 2004, *AJ*, 128, 1929  
Zhang X., Zhao G., Zheng Y. G., Ma L., Xie Z. H., Hu S. M., 2007, *AJ*, 133, 1995

This paper has been typeset from a  $\text{\TeX}/\text{\LaTeX}$  file prepared by the author.